Volume 1 | Number 1 | Jan 2013 | Pages 1–100

PCCP

Physical Chemistry Chemical Physics
www.rsc.org/pccp

ROYAL SOCIETY OF CHEMISTRY

ROYAL SOCIETY OF CHEMISTRY

Journal Name

ARTICLE TYPE

Controlling electron emission from the photoactive yellow protein chromophore by substitution at the coumaric acid group†

Michael A. Parkes, Ciara Phillips, Michael J. Porter and Helen H. Fielding*

Understanding how the interactions between a chromophore and its surrounding protein control the function of a photoactive protein remains a challenge. Here, we present the results of photoelectron spectroscopy measurements and quantum chemistry calculations aimed at investigating how substitution at the coumaryl tail of the photoactive yellow protein chromophore controls competing relaxation pathways following photoexcitation of isolated chromophores in the gas phase with ultraviolet light in the range $350 - 315$ nm. The photoelectron spectra are dominated by electrons resulting from direct detachment and fast detachment from the $2^1\pi\pi^*$ state but also have a low electron kinetic energy component arising from autodetachment from lower lying electronically excited states or thermionic emission from the electronic ground state. We find that substituting the hydrogen atom of the carboxylic acid group with a methyl group lowers the threshold for electron detachment but has very little effect on the competition between the different relaxation pathways, whereas substituting with a thioester group raises the threshold for electron detachment and appears to 'turn off' the competing electron emission processes from lower lying electronically excited states. This has potential implications in terms of tuning the light-induced electron donor properties of photoactive yellow protein.

1 Introduction

Photoactive proteins are exploited widely in nature and technology to make systems responsive to light. At the heart of a photoactive protein is a small molecule chromophore that absorbs the light. One photoactive protein that continues to attract a great deal of attention is photoactive yellow protein (PYP), the photoreceptor that is responsible for the negative phototaxis of the *Halorhodospira halophila* bacterium.[1–4] The small molecule chromophore in PYP is a deprotonated *para*-coumaric acid anion (pCA$^-$) and it is linked to the protein by a thioester covalent bond to a cysteine residue, Cys69 (Fig. 1). In PYP, the negative charge on the chromophore is stabilised by a network of hydrogen-bonds involving Cys69, Glu46, Tyr42 and Thr50 residues and a positively charged Arg52 residue. Following absorption of a photon, the chromophore undergoes rapid *trans-cis* isomerisation, the hydrogen-bond network then reorganises to accommodate the *cis* conformation and the protein unfolds and protonates.[5–8] Subsequent *cis-trans* isomerisation of the chromophore, refolding

of the protein and deprotonation, completes the photocycle. In the absence of chromophore-protein interactions, in solution and in the denatured protein, the chromophore does not form a stable *cis* intermediate but relaxes back to the ground state from a twisted *trans* conformation.[9] Understanding how the interactions between the chromophore and the surrounding protein control the dynamical pathway of the chromophore, and thus the protein function, is a major challenge in photochemistry and photobiology.

There have been numerous experimental investigations of the spectroscopy and excited state dynamics of isolated model PYP chromophores, in the gas-phase and in solution, aimed at disentangling the roles of the chromophore and the protein.[9–27]. Action spectra of the deprotonated coumaric acid anion in the gas-phase have been found to have a maximum around 430 nm, which is reasonably close to the absorption maximum of PYP (446 nm)[21] and it is now generally accepted that this similarity is the combined effect of numerous chromophore-protein interactions. Although the absorption spectra of the gas-phase chromophore and PYP are similar, time-resolved measurements of a deprotonated methyl terminated ketone analogue of the PYP chromophore in the gas-phase, excited at 400 nm (3.1 eV), revealed that 80% of the excited state population relaxed back to the ground state on a timescale of 52 ps via a twisted intermediate, similar to isolated

---

a Department of Chemistry, University College London, 20 Gordon Street, London WC1H 0AJ, UK. E-mail: h.h.fielding@ucl.ac.uk

† Electronic Supplementary Information (ESI) available: Synthesis of *S*-methyl (*E*)-3-(4-hydroxyphenyl)prop-2-enethioate (*p*CT). Coordinates of the optimised geometries of the deprotonared anions. See DOI: 10.1039/b000000x/
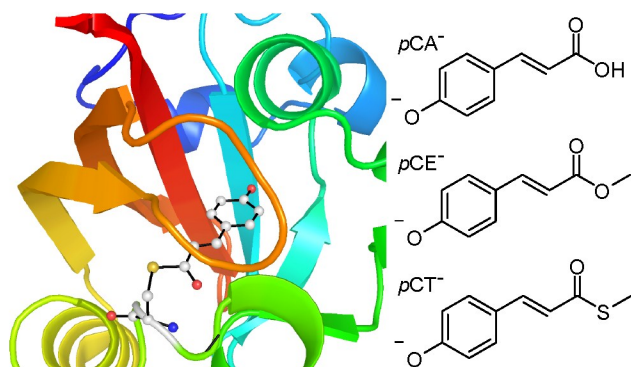
Fig. 1 Left: PYP chromophore in its protein environment (Protein Data Bank). Right: Structures of the deprotonated PYP chromophores employed in this work.

chromophores in solution, and that the remaining 20% of the excited state population underwent autodetachment (electron emission).[16] From this, the authors concluded that one of the roles of the protein environment was to funnel the excited state population through the S_1/S_0 conical intersection seam to the *cis* isomer and to suppress electron emission. It is worth noting that electron emission has also been observed in isolated chromophores in aqueous solution[12] and in PYP[28] at higher photoexcitation energies. Interestingly, the spectrum of the electron emitted from the chromophore in PYP was found to be similar to that of a solvated electron, suggesting that the protein pocket provides a local environment for an electron that is similar to water.

Studies of numerous chromophore analogues in aqueous solution have found that the substituent on the coumaryl tail of the chromophore plays a key role in the excited state dynamics, highlighting the significance of the thioester link to the Cys69 amino acid residue. These studies found that derivatives with strong electron accepting groups, such as thioesters, return to the initial *trans* configuration on timescales of ~ 1 ps, whereas those with weak electron accepting groups, such as amides or carboxylate, have longer excited state lifetimes, up to 10 ps for the carboxylate, and measurable *trans-cis* isomerisation yields.[9,11,12,18]

From a theoretical perspective, there have been numerous studies of PYP and the PYP chromophore, in the gas-phase and in solution, aimed at investigating the role of the environment on its electronic structure and dynamics.[29–37] Various strategies have been employed, ranging from studies of a few solvent molecules or the closest protein residues to quantum-mechanical/molecular mechanics and averaged solvent electrostatic potential/molecular dynamics methods. Such studies have highlighted the importance of torsions around the C–C single bond between the phenoxide ring and the C=C double bond in controlling the *trans-cis* isomerisation process in the protein.[29] They have also rationalised the blue solvatochromic shift of pCA$^-$ and its derivatives in terms of a transfer of electron density from the phenolate end of the chromophore to the rest of the chromophore, resulting in a decrease in dipole moment between the ground and first electronically excited states.[34] García-Prieto and coworkers have recently reported a detailed theoretical study of the absorption

spectra of different chromophore analogues in the gas-phase and solution and found that the presence of a sulfur atom on the coumaryl tail modulates the solvent effect for the first few excited electronic states[37] which could explain the differences observed in the excited state dynamics in aqueous solution discussed above.[9,11,12,18]

In a previous anion photoelectron spectroscopy study of gas-phase pCA$^-$ and its *ortho*- and *meta*- isomers, we found that moving the position of the O$^-$ group on the phenoxide group of the chromophore controlled the competition between electron emission and internal conversion.[27] The focus of this paper is to determine whether the thioester link also plays a role in controlling the competition between electron emission and internal conversion in the gas-phase. We employ a combination of anion photoelectron spectroscopy and quantum chemistry calculations to investigate the effect of substituting the hydrogen atom of the carboxylic acid group with a methyl group and substituting the oxygen atom of the methoxy group with a sulfur atom. Specifically, we excite pCA$^-$, its methyl ester, pCE$^-$, and its methyl thioester, pCT$^-$, (Fig. 1) with ultraviolet light in the range 350–315 nm (3.54–3.94 eV), within the $2^1\pi\pi^* \leftarrow S_0$ absorption band. Improving our understanding of the role of the thioester link in controlling electron emission in PYP may provide a basis for practical applications such as the rational design of photoactive materials with specific redox properties.

2 Experimental and Computational Methods

2.1 Chromophores

pCA was purchased from Sigma-Aldrich and pCE was purchased from Tokyo Chemical Industry, both were used without further purification. pCT was synthesised by a modification of the method of Naseem *et al.*[26] (Supplementary Information).

2.2 Photoelectron spectroscopy

Photoelectron spectra were recorded using our photoelectron imaging apparatus that has been described elsewhere.[27,38–40] Briefly, deprotonated anions of pCA, pCE or pCT were generated by electrospray ionisation of ~ 1 mM solutions of the chromophores in methanol, with a few drops of aqueous ammonia. The pCA$^-$, pCE$^-$ or pCT$^-$ anions were mass-selected by a quadrupole and passed into a collision cell doubling as a hexapole ion-trap. The anions were released from the trap at a frequency of 20 Hz, to match the repetition rate of the laser system, and transported to the interaction region of collinear velocity-map imaging optics. In the interaction region, the ion packet was crossed with nanosecond laser pulses of wavelength 315, 320 and 350 nm, generated by frequency doubling the output of a Nd:YAG pumped dye laser. Electrons generated by the laser pulse were then accelerated towards a position sensitive detector and imaged using a phosphor screen and CCD camera. Laser-only images were subtracted from images recorded following the interaction of the laser light with the anions, to eliminate background counts arising from scattered laser light and ionisation of residual gas. The photoelectron images were inverted using the pBASEX method.[41]

The wavelength of the laser light was measured using a waveme-ter and the energy scale of the detector was calibrated by record-ing the photoelectron spectrum of I^-. The energy resolution is $\sim 5\%$ and the error in electron kinetic energy is around ± 0.05 eV.

2.3   Calculations

All electronic structure calculations were performed using the Gaussian09 suite of programmes.[42] The geometric structures of the phenolate form of pCE$^-$, pCT$^-$ and pCA$^-$, and correspond-ing neutral radicals, were optimised using the B3LYP hybrid func-tional[43–46] and a 6-311++G(3df,3pd) basis set.[47–49] Frequency calculations were performed to ensure that the optimised struc-tures were true minima.

Vertical excitation energies (VEEs) of the singlet excited electronic states of the phenolate deprotonated coumaric acid chromophores were calculated using the CAM-B3LYP/6-311++G(3df,3pd) method. The long-range corrected version of B3LYP using the Coulomb Attenuating Method (CAM)[50] was cho-sen for its potential to describe excited states with charge-transfer character and because it has been shown to yield reasonable re-sults for the phenolate form of the pCA$^-$ anion.[22]

Vertical detachment energies (VDEs) were determined using electron propagator theory (EPT)[51,52] and a 6-311++G(3df,3pd) basis set. We have already benchmarked this approach against the high-resolution photoelectron spectrum of the phenoxide an-ion and shown that it yields good results for the deprotonated green fluorescent protein chromophore anion.[40] Adiabatic de-tachment energies (ADEs) were determined using the B3LYP/6-311++G(3df,3pd) method, $\text{ADE} = E_{min}^{radical} + E_{ZPE}^{radical} - [E_{min}^{anion} + E_{ZPE}^{anion}]$, where subscripts 'min' and 'ZPE' represent the minimum energy and zero-point energies, respectively. Higher VDEs were determined by calculating the VEEs of the first electronically ex-cited doublet states of the neutral radicals at the optimised ge-ometries of the corresponding anions using the CAM-B3LYP/6-311++G(3df,3pd) method and adding these to the VDEs calcu-lated using the EPT method.

3   Results and Discussion

Photoelectron spectra of the deprotonated coumaric acid anion (pCA$^-$), an ester analogue (pCE$^-$) and a thioester analogue (pCT$^-$) (Fig. 1) were recorded as a function of electron kinetic energy (eKE) and are presented as a function of electron binding energy, eBE $= h\nu - $ eKE in Fig. 2.
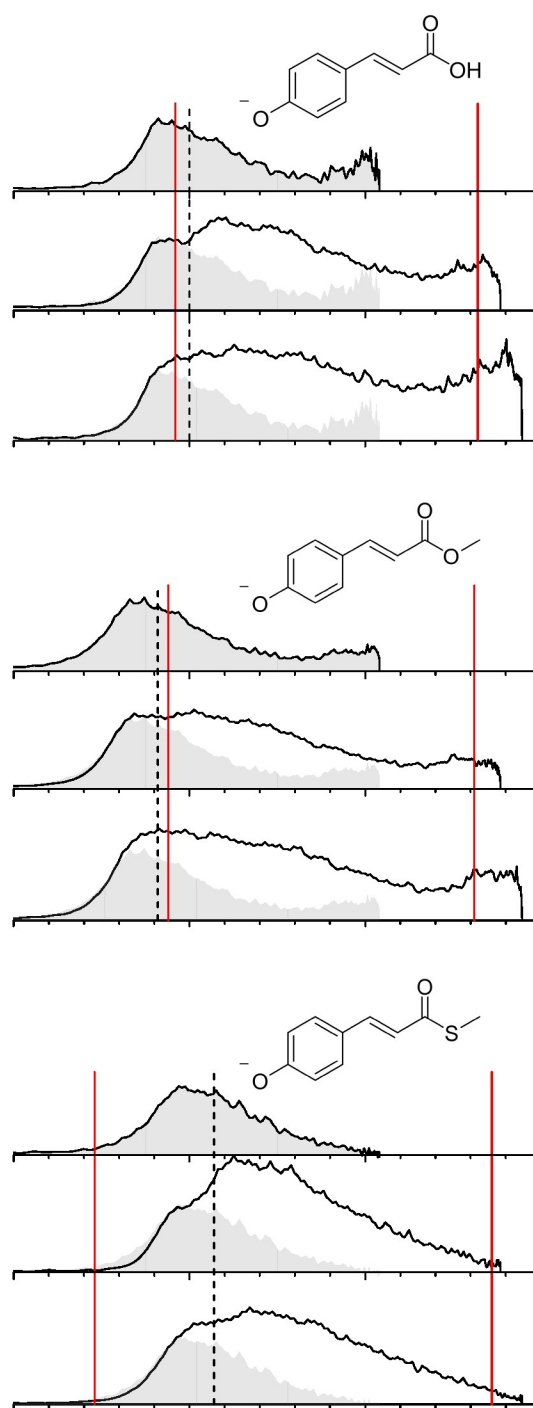
Fig. 2 Photoelectron spectra of pCA$^-$, pCE$^-$ and pCT$^-$ recorded at 350 nm (3.54 eV), 320 nm (3.87 eV) and 315 nm (3.94 eV) (solid black lines). The 350 nm photoelectron spectra (shaded grey) are superimposed on photoelectron spectra recorded at shorter wavelengths, whose intensities have been scaled so the rising edges are aligned. Dashed black lines mark the calculated VDEs (Table 1) and solid red lines mark the calculated VEEs determined by García-Prieto and coworkers for the two lowest energy singlet $\pi\pi^*$ states,[37] listed in Table 2.

All the photoelectron spectra are dominated by broad, unre-

Table 1 EPT/6-311++G(3df,3pd) calculated vertical detachment energies (VDEs) and pole strengths (in parentheses), B3LYP/6-311++G(3df,3pd) D_0-S_0 adiabatic detachment energies (ADEs) (0-0 transition) and maxima of the experimental 350 nm photoelectron spectra (all in eV) for the phenolate form of pCA$^-$, pCE$^-$ and pCT$^-$.

Chromophore	VDE	ADE (0-0)	Expt
pCA$^-$	3.00 (0.879)	2.99	2.91±0.05
pCE$^-$	2.91 (0.875)	2.91	2.83±0.05
pCT$^-$	3.07 (0.879)	3.03	2.96±0.05

solved features at low eBEs. The rising edges of these broad features remain at constant eBE for all photon energies and are therefore attributed to direct photodetachment (PD). The maxima of the 350 nm (3.54 eV) spectra are in good agreement (~ 0.1 eV) with the calculated vertical detachment energies (VDEs) and adiabatic detachment energies (ADEs), which are presented in Table 1. It is worth noting that there is significant photoelectron emission at lower eBEs than the calculated VDEs and ADEs in all the photoelectron spectra. In pCA$^-$, and one of its isomers oCA$^-$, this has been attributed to rotation around the single bond between the C=C double bond and the phenoxide group, so we assume these torsional motions play a similar role in pCE$^-$ and pCT$^-$. The fact that the calculated VDEs and ADEs are so close to one another suggests that the minimum energy geometries of the anion and the radical are very similar, in agreement with the results of our combined photoelectron spectroscopy and computational study of gas-phase pCA$^-$ and its *ortho-* and *meta-* isomers.[27] Our calculated VDEs are also in good agreement with the EOM-IP-CCSD/6-311+G(df,pd) value reported by Zuev *et al.* for pCA$^-$ (2.92 eV),[53] the OVGF/aug-cc-pVDZ value reported by Gromov *et al.* for pCT$^-$ (2.90 eV)[30] and the experimental VDE reported for the methyl ketone analogue (2.9 eV).[16]

It is worth noting that pCA$^-$ can be formed during electrospray ionisation as a carboxylate anion or as a phenolate anion, whereas pCE$^-$ and pCT$^-$ have only one deprotonation site and can only be formed as phenolate anions. It is clear from the photoelectron spectra (Fig. 2) that all three chromophores have similar VDEs (around 3 eV), which supports our earlier suggestion that pCA$^-$ is formed in its phenolate form in our instrument when using methanol with a few drops of aqueous ammonia as a solvent.[27] This contrasts with the observations of Almasian *et al.*,[25] but perhaps emphasises the importance of instrumental parameters, such as the position of the electrospray head, as well as choice of solvent in determining the deprotonation site.[54] The VDE for the carboxylate form of pCA$^-$ (4.68 eV)[27] is significantly higher than for the phenolate form so it is also possible that both phenolate and carboxylate forms are present in our instrument but that we are only sensitive to the phenolate form in experiments with photons < 4 eV.

Although the VDEs of the chromophores are similar, the maxima in the photoelectron spectra and calculated VDEs (Table 1) increase in the order pCE$^-$ < pCA$^-$ < pCT$^-$. This trend can be understood in terms of the stabilising effect of electron accepting substituents lowering the energy of the resonantly stabilised anions as the electron affinity increases in the order OMe < OH <

SMe.

The calculated vertical excitation energies for the first two $^1\pi\pi^*$ states and the first ^{1}nπ^* state of pCA$^-$, pCE$^-$ and pCT$^-$ are listed in Table 2, alongside the results of higher-level SA-CASSCF(14,12)-PT2/cc-pVDZ calculations by García-Prieto and coworkers[37] and experimental values reported by Rocha-Rinza and coworkers.[21] The molecular orbitals involved in the transitions are plotted in Fig. 3. Our calculated value for pCE$^-$ is consistent with that calculated using the CAM-B3LYP/aug-cc-pVTZ method[22] and our value for pCA$^-$ lies within the range of values calculated by Zuev *et al.*[53] and Uppsten and Durbeej,[55] although all the values are ~ 0.5 eV higher than the experimental values determined from action spectra[21] and those calculated using the SA-CASSCF(14,12)-PT2/cc-pVDZ method.[37] Nonetheless, the characters of the excited states calculated using the CAM-B3LYP/6-311++G(3df,3pd) method, and the energies of the excited states with respect to one another, are in good agreement with those calculated using the SA-CASSCF(14,12)-PT2/cc-pVDZ method. To guide our interpretation of the photoelectron spectra, we have marked the more accurate VEEs determined by García-Prieto and coworkers using the SA-CASSCF(14,12)-PT2/cc-pVDZ method[37] on our experimental spectra (Fig. 2) and use the configurations obtained from the CAM-B3LYP/6-311++G(3df,3pd) to determine the characters of the excited states with respect to the detachment continua.

The effect of substituting the hydrogen on the carboxylic acid group in pCA$^-$ for a methyl group (pCE$^-$) has very little effect on any of the VEEs. However, substituting the oxygen atom for a sulfur atom (pCT$^-$) causes the $1^1\pi\pi^*$ and 1^1nπ^* states to red-shift by $0.1 - 0.2$ eV, although it has very little effect on the $2^1\pi\pi^*$ state. These observations can be understood in terms of the molecular orbitals involved in the transitions (Fig. 3). Transitions to the $1^1\pi\pi^*$ and 1^1nπ^* states are to the π_1^* molecular orbital, which is delocalised across the anion and therefore stabilised by the electron accepting methyl thioester group, whereas the $2^1\pi\pi^*$ transition is to the π_2^* molecular orbital, which is localised on the phenoxide group and is barely influenced by changing the substituents on the coumaryl tail.

It is clear from Fig. 2 that the $1^1\pi\pi^*$ and D_0 states are very close to one another in pCA$^-$ and pCE$^-$, but that the $1^1\pi\pi^*$ state is $0.2 - 0.3$ eV lower in energy than the D_0 state in pCT$^-$. This suggests that the thioester link between the chromophore and the protein plays a role in ensuring that the $1^1\pi\pi^*$ state is bound with respect to photodetachment following excitation at the maximum of $1\pi\pi^* \leftarrow S_0$ absorption band. This is consistent with the fact that there have not been any reports of electron emission from PYP following excitation within the $1\pi\pi^* \leftarrow S_0$ absorption maximum at 446 nm (2.78 eV), even though electron emission has been observed following excitation at higher photon energies.[28]

As the photon energy increases, the broad features in the photoelectron spectra change shape on the high eBE side, characteristic of an indirect PD process following resonant excitation of a higher lying electronically excited state (autodetachment). In pCA$^-$, and one of its isomers mCA$^-$, this broadening has already been rationalised in terms of resonant excitation of higher-lying $2^1\pi\pi^*$ excited states followed by autodetachment.[27] Similar ef-

Table 2 CAM-B3LYP/6-311++G(3df,3pd) vertical excitation energies in eV and oscillator strengths f (in parentheses) for the phenolate form of pCA⁻, pCE⁻ and pCT⁻ compared with SA-CASSCF(14,12)-PT2/cc-pVDZ calculated values[37] and experimental values[21] from the literature

Chromophore	$1^1\pi\pi^*$	$1^1n\pi^*$	$2^1\pi\pi^*$	$1^1\pi\pi^{*\,37}$	$1^1n\pi^{*\,37}$	$2^1\pi\pi^{*\,37}$	Expt[21]
pCA⁻	3.45 (0.91)	4.09 (0.00)	4.33 (0.10)	2.96	3.65	3.82	2.89
pCE⁻	3.43 (0.95)	4.12 (0.00)	4.31 (0.11)	2.94	3.65	3.81	2.88
pCT⁻	3.30 (1.12)	4.00 (0.00)	4.34 (0.09)	2.73	3.47	3.86	-
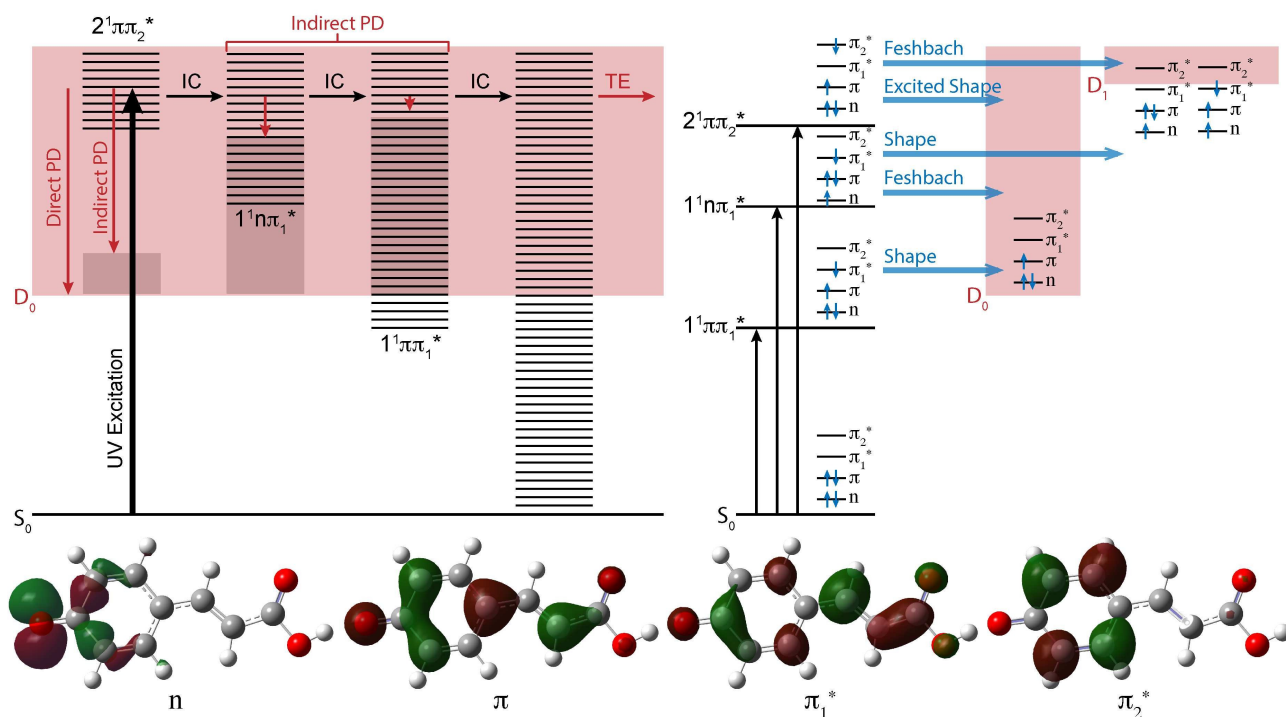
Fig. 3 Top left: Jablonski diagram illustrating the electronic relaxation and emission processes following UV photoexcitation of pCA⁻, pCE⁻ and pCT⁻. Horizontal black lines represent the vibrational levels of the excited electronic states and the solid pink area represents the electron detachment continuum. Vertical red arrows represent the eKE of direct and indirect electron emission processes and the solid grey areas represent the vibrational energy left in the neutral radical after electron detachment (determined by the propensity for conservation of vibrational energy). The horizontal black arrows represent some of the possible internal conversion (IC) processes and the horizontal red arrow represents electrons with eKE ~ 0 eV following thermionic emission (TE) from vibrationally hot S_0. Top right: Schematic energy level diagram showing the resonance character (horizontal blue arrows) of the first three excited singlet electronic states of the chromophores with respect to the D_0 and D_1 electronic continua. Bottom: Main CAM-B3LYP/6-311++G(3df,3pd) molecular orbitals involved in the transitions to the first three excited singlet electronic states.

fects have also been observed in photoelectron spectra of the deprotonated green fluorescent protein (GFP) chromophore following resonant excitation of higher lying excited $^1\pi\pi^*$ states.[40,56,57]

The 350 nm (3.54 eV) photoelectron spectra are least influenced by resonant excitation of the $2^1\pi\pi^*$ states, which have VEEs around $3.8 - 3.9$ eV for all three chromophores (Fig. 2), so the 350 nm spectra have been superimposed on the 320 nm and 315 nm photoelectron spectra to highlight the contributions from resonant excitation of the $2^1\pi\pi^*$ states in the photoelectron spectra recorded at shorter wavelengths. The difference is most pronounced for the 320 nm photoelectron spectrum of pCT$^-$, when the photon energy (3.87 eV) is resonant with the $2\pi\pi^* \leftarrow S_0$ absorption maximum (3.86 eV[37]).

In Fig. 3, the possible electronic relaxation and electron emission processes following photoexcitation of pCA$^-$, pCE$^-$ and pCT$^-$ are illustrated on a Jablonski diagram and the resonance characters of the first three singlet excited electronic states with respect to the D_0 and D_1 electronic continua are also shown. The $2^1\pi\pi^*$ state responsible for the broadening on the high eBE edges of the photoelectron spectra (Fig. 2) is an excited shape resonance with respect to the D_0 continuum, implying a strong coupling between the $2^1\pi\pi^*$ state and the D_0 continuum and fast electron emission.

The photoelectron spectra of pCA$^-$ and pCE$^-$ also have features at high eBE (low eKE) that shift towards higher eBEs as the photon energy increases, characteristic of indirect PD processes. Interestingly, this feature is not observed in the photoelectron spectra of pCT$^-$. The first question to ask is whether the D_1 continua are accessible energetically. The VDEs to the first electronically excited states of the neutral radicals have been calculated to be 4.38, 4.32 and 4.50 eV for pCA$^-$, pCE$^-$ and pCT$^-$, respectively. The calculated VDEs are higher than the photon energies used in our experiments; however, it is possible that they are overestimated by ~ 0.5 eV, similar to the VEEs calculated for the anion using the same method (Table 2), in which case the D_1 continuum would be accessible energetically in pCA$^-$ and pCE$^-$ at 320 and 315 nm and at 350 nm if the ADEs were $0.3 - 0.4$ eV lower than the VDEs. The next question to ask is if any of the excited states of pCA$^-$ and pCE$^-$ are coupled strongly to the D_1 continuum. The $2^1\pi\pi^*$ state is a Feshbach resonance with respect to the D_1 continuum, implying a weak coupling between the $2^1\pi\pi^*$ state and the D_1 continuum and slow electron emission. Thus, indirect electron emission from the $2^1\pi\pi^*$ state to the D_1 continuum is unlikely to compete with fast electron emission to the D_0 continuum. However, ultrafast internal conversion to a lower lying excited electronic state may compete with the fast electron emission to the D_0 continuum. Subsequent electron emission from lower lying electronically excited states could generate low eKE electrons, if the displacements between the minima of these states and the D_0 state were sufficiently small that the Franck-Condon factors were largest between the high vibrational levels of the electronically excited states and high vibrational levels of D_0 (Fig. 3). The $1^1n\pi^*$ state has shape resonance character with respect to the D_1 continuum and Feshbach character with respect to the D_0 continuum, whereas the $1^1\pi\pi^*$ state has shape resonance character with respect to the D_0 detachment continuum and Feshbach character

with respect to the D_1 continuum. Consequently, it seems likely that any population relaxing to the $1^1n\pi^*$ state would undergo fast electron emission to the D_1 continuum or internal conversion to $1^1\pi\pi^*$ or S_0 states and any population relaxing to the $1^1\pi\pi^*$ state would undergo fast electron emission to the D_0 continuum or internal conversion to S_0. Internal conversion processes populating high vibrational levels of the electronic ground state of the anion would also result in low eKE electrons from thermionic emission (Fig. 3).

It is possible that the low eKE (high eBE) electrons observed in the 350 nm photoelectron spectra of pCA$^-$ and pCE$^-$ arise from a different relaxation process than those in the 320 nm and 315 nm photoelectron spectra. The action absorption spectrum for pCE$^-$ shows that 350 nm lies between the $1^1\pi\pi^*$ and $2^1\pi\pi^*$ absorption bands,[22] so the non-zero absorption could be the result of populating high lying vibrational levels of the $1^1\pi\pi^*$ state which could then autodetach to the D_0 continuum or undergo internal conversion to S_0 followed by thermionic emission.

Thus, the presence of high eBE (low eKE) electrons in the 315 nm and 320 nm photoelectron spectra of pCA$^-$ and pCE$^-$, that shift towards higher eBEs as the photon energy increases, suggests that IC to lower lying electronic states or the ground electronic state compete with PD. The presence of high eBE (low eKE) electrons in the 350 nm photoelectron spectra of pCA$^-$ and pCE$^-$ can either be attributed to a similar process or to resonant excitation of the $1^1\pi\pi^*$ state followed by autodetachment or internal conversion to the ground state and thermionic emission. The absence of high eBE (low eKE) electrons in the 315 nm and 320 nm photoelectron spectra of pCT$^-$ could be the result of raising the threshold for detachment into the D_1 continuum and 'turning off' the $1^1n\pi^* \rightarrow D_1 + e^-$ detachment channel. However, if this were the case, subsequent electronic relaxation from the $1^1n\pi^*$ state to the $1^1\pi\pi^*$ or S_0 states would themselves generate low eKE electrons by fast electron detachment into the D_0 continuum or thermionic emission. A more likely explanation seems to be that lowering the $1^1n\pi^*$ and $1^1\pi\pi^*$ states in the Franck-Condon region makes conical intersections between the $2^1\pi\pi^*$ and $1^1n\pi^*$ or $1^1\pi\pi^*$ states inaccessible or less accessible, effectively 'turning off' internal conversion to these states and the ground electronic state, leaving indirect electron emission from the $2^1\pi\pi^*$ state to the D_0 continuum as the only relaxation pathway. The absence of high eBE (low eKE) electrons in the 350 nm photoelectron spectrum of pCT$^-$ can be explained either as 'turning off' internal conversion processes from the low vibrational levels of the $2^1\pi\pi^*$ state or 'turning off' autodetachment and internal conversion from high vibrational levels of the $1^1\pi\pi^*$ state. This opens the interesting possibility of using changes to the link between the chromophore and the protein in PYP to manipulate the UV induced electron donor properties of the protein and isolated chromophores, with the potential to monitor and manipulate redox processes.[58]

4 Conclusions

In this paper, we have used photoelectron spectroscopy and quantum chemistry calculations to investigate the role of the thioester group in controlling the competition between internal conver-

sion and electron emission in isolated PYP chromophores in the gas phase. Following photoexcitation with ultraviolet light in the range $350 - 315$ nm, we see photoelectrons with high eKEs that arise from direct photodetachment or from excitation of the $2^1\pi\pi^*$ state followed by indirect photodetachment to the D_0 continuum. We also see photoelectrons with low eKEs that appear to arise from an indirect electron emission process. We attribute these low eKE electrons to photodetachment from lower lying $1^1n\pi^*$ or $1^1\pi\pi^*$ states or to the vibrationally hot electronic ground state and subsequent thermionic emission. We find that substituting the hydrogen atom of the carboxylic acid group with a methyl group lowers the vertical detachment energy but has very little effect on the competition between internal conversion to lower lying electronic states and electron emission, whereas substituting with a thioester group raises the vertical detachment energy and appears to 'turn off' competing electron emission processes from lower lying electronically excited states or the electronic ground state. This suggests that one of the roles of the thioester link between the chromophore and the protein is to contribute to impeding electron emission following photoexcitation of the $1\pi\pi^*$ state and another is to 'turn off' competing relaxation pathways to allow the chromophore to act as an efficient light-induced electron donor following photoexcitation at shorter wavelengths within the $2^1\pi\pi^* \leftarrow S_0$ absorption band.

5 Acknowledgements

References

1 T. E. Meyer, *Biochim. Biophys. Acta*, 1985, **806**, 175–183.

2 W. W. Sprenger, W. D. Hoff, J. P. Armitage and K. J. Hellingwerf, *J. Bacteriol.*, 1993, **175**, 3096–3104.

3 K. J. Hellingwerf, J. Hendriks and T. Gensch, *J. Phys. Chem. A*, 2003, **107**, 1082–1094.

4 F. Schotte, H. S. Cho, V. R. I. Kaila, H. Kamikubo, N. Dashdorj, E. R. Henry, T. J. Graber, R. Henning, M. Wulff, G. Hummer, M. Kataoka and P. A. Anfinrud, *Proc. Natl. Acad. Sci. U. S. A.*, 2012, **109**, 19256–19261.

5 R. Kort, H. Vonk, X. Xu, W. D. Hoff, W. Crielaard and K. J. Hellingwerf, *FEBS Lett.*, 1996, **382**, 73–78.

6 U. K. Genick, S. M. Soltis, P. Kuhn, I. L. Canestrelli and E. D. Getzoff, *Nature*, 1998, **392**, 206–209.

7 A. Xie, W. D. Hoff, A. R. Kroon and K. J. Hellingwerf, *Biochemistry*, 1996, **35**, 14671–14678.

8 M. Unno, M. Kumauchi, J. Sasaki, F. Tokunaga and S. Yamauchi, *J. Am. Chem. Soc.*, 2000, **12**, 4233–4234.

9 P. Changenet-Barret, A. Espagne, P. Plaza, K. J. Hellingwerf and M. M. Martin, *New J. Chem.*, 2005, **29**, 527.

10 P. Changenet-Barret, P. Plaza and M. M. Martin, *Chem. Phys. Lett.*, 2001, **336**, 439–444.

11 D. S. Larsen, M. Vengris, I. H. van Stokkum, M. A. van der Horst, R. A. Cordfunke, K. J. Hellingwerf and R. van Grondelle, *Chem. Phys. Lett.*, 2003, **369**, 563–569.

12 D. S. Larsen, M. Vengris, I. H. M. van Stokkum, M. A. van der Horst, F. L. de Weerd, K. J. Hellingwerf and R. van Grondelle, *Biophys. J.*, 2004, **86**, 2538–50.

13 D. S. Larsen, I. H. M. van Stokkum, M. Vengris, M. A. van der Horst, F. L. de Weerd, K. J. Hellingwerf and R. van Grondelle, *Biophys. J.*, 2004, **87**, 1858–1872.

14 I. B. Nielsen, S. Boye-Peronne, M. O. A. El Ghazaly, M. B. Kristensen, S. Brondsted Nielsen and L. H. Andersen, *Biophys. J.*, 2005, **89**, 2597–2604.

15 M. Vengris, D. S. Larsen, M. A. van der Horst, O. F. A. Larsen, K. J. Hellingwerf and R. van Grondelle, *J. Phys. Chem. B*, 2005, **109**, 4197–208.

16 I.-R. Lee, W. Lee and A. H. Zewail, *Proc. Natl. Acad. Sci. U. S. A.*, 2006, **103**, 258–262.

17 A. Espagne, D. H. Paik, P. Changenet-Barret, M. M. Martin and A. H. Zewail, *ChemPhysChem*, 2006, **7**, 1717–1726.

18 A. Espagne, P. Changenet-Barret, J. B. Baudin, P. Plaza and M. M. Martin, *J. Photochem. Photobiol. A Chem.*, 2007, **185**, 245–252.

19 A. Espagne, D. H. Paik, P. Changenet-Barret, P. Plaza, M. M. Martin and A. H. Zewail, *Photochem. Photobiol. Sci.*, 2007, **6**, 780–787.

20 L. Lammich, J. Rajput and L. H. Andersen, *Phys. Rev. E*, 2008, **78**, 051916.

21 T. Rocha-Rinza, O. Christiansen, J. Rajput, A. Gopalan, D. B. Rahbek, L. H. Andersen, A. V. Bochenkova, A. A. Granovsky, K. B. Bravaya, A. V. Nemukhin, K. L. Christiansen and M. Brondsted Nielsen, *J. Phys. Chem. A*, 2009, **113**, 9442–9449.

22 T. Rocha-Rinza, O. Christiansen, D. B. Rahbek, B. Klærke, L. H. Andersen, K. Lincke and M. Brøndsted Nielsen, *Chem. Eur. J.*, 2010, **16**, 11977–11984.

23 J. Rajput, D. B. Rahbek, G. Aravind and L. H. Andersen, *Biophys. J.*, 2010, **98**, 488–492.

24 H. Kuramochi, S. Takeuchi and T. Tahara, *J. Phys. Chem. Lett.*, 2012, **3**, 2025–2029.

25 M. Almasian, J. Grzetic, J. Van Maurik, J. D. Steill, G. Berden, S. Ingemann, W. J. Buma and J. Oomens, *J. Phys. Chem. Lett.*, 2012, **3**, 2259–2263.

26 S. Naseem, A. D. Laurent, E. C. Carroll, M. Vengris, M. Kumauchi, W. D. Hoff, A. I. Krylov and D. S. Larsen, *J. Photochem. Photobiol. A Chem.*, 2013, **270**, 43–52.

27 C. R. S. Mooney, M. A. Parkes, A. Iskra and H. H. Fielding, *Angew. Chem. Int. Ed.*, 2015, **54**, 5646–5649.

28 J. Zhu, L. Paparelli, M. Hospes, J. Arents, J. T. M. Kennis, I. H. M. van Stokkum, K. J. Hellingwerf and M. L. Groot, *J. Phys. Chem. B*, 2013, **117**, 11042–11048.

29 G. Groenhof, M. Bouxin-cademartory, B. Hess, S. P. D. Visser, H. J. C. Berendsen, M. Olivucci, A. E. Mark and M. A. Robb, *J. Am. Chem. Soc.*, 2004, **126**, 4228–4233.

30 E. V. Gromov, I. Burghardt, J. T. Hynes, H. Köppel and L. S. Cederbaum, *J. Photochem. Photobiol. A Chem.*, 2007, **190**,

241–257.

31 D. Zuev, K. B. Bravaya, M. V. Makarova and A. I. Krylov, *J. Chem. Phys.*, 2011, **135**, 194304.

32 E. V. Gromov, I. Burghardt, H. Köppel and L. S. Cederbaum, *J. Phys. Chem. A*, 2011, **115**, 9237–9248.

33 M. Boggio-Pasqua, M. A. Robb and G. Groenhof, *J. Am. Chem. Soc.*, 2009, **131**, 13580–13581.

34 F. F. García-Prieto, I. F. Galván, A. Muñoz Losa, M. A. Aguilar and M. E. Martín, *J. Chem. Theory Comput.*, 2013, **9**, 4481–4494.

35 E. V. Gromov, *J. Chem. Phys.*, 2014, **141**, 224308.

36 S. Frutos-Puerto, A. Muñoz Losa, M. E. Martín and M. A. Aguilar, *Comput. Theor. Chem.*, 2014, **1040-1041**, 287–294.

37 F. F. García-Prieto, M. A. Aguilar, F. J. Olivares del Valle, I. Fernández Galván, A. Muñoz Losa, M. L. Sánchez and M. E. Martín, *J. Phys. Chem. A*, 2015, **119**, 5504–5514.

38 A. R. McKay, M. E. Sanz, C. R. S. Mooney, R. S. Minns, E. M. Gill and H. H. Fielding, *Rev. Sci. Instrum.*, 2010, **81**, 123101.

39 C. R. S. Mooney, M. E. Sanz, A. R. McKay, R. J. Fitzmaurice, A. E. Aliev, S. Caddick and H. H. Fielding, *J. Phys. Chem. A*, 2012, **116**, 7943–7949.

40 C. R. S. Mooney, M. A. Parkes, L. Zhang, H. C. Hailes, A. Simperler, M. J. Bearpark and H. H. Fielding, *J. Chem. Phys.*, 2014, **140**, 205103.

41 G. A. Garcia, L. Nahon and I. Powis, *Rev. Sci. Instrum.*, 2004, **75**, 4989.

42 M. J. Frisch, G. W. Trucks, H. B. Schlegel, G. E. Scuseria, M. A. Robb, J. R. Cheeseman, G. Scalmani, V. Barone, B. Mennucci, G. A. Petersson, H. Nakatsuji, M. Caricato, H. P. H. X. Li, A. F. Izmaylov, J. Bloino, G. Zheng, J. L. Sonnenberg, M. Hada, M. Ehara, K. Toyota, R. Fukuda, J. Hasegawa, M. Ishida, T. Nakajima, Y. Honda, O. Kitao, H. Nakai, T. Vreven, J. A. M. Jr., J. E. Peralta, F. Ogliaro, M. J. Bearpark, J. J. Heyd, E. Brothers, K. N. Kudin, V. N. Staroverov, T. Keith, R. Kobayashi, J. Normand, K. Raghavachari, A. Rendell, J. C. Burant, S. S. Iyengar, J. Tomasi, M. Cossi, N. Rega, J. M. Millam, M. Klene, J. E. Knox, J. B. Cross, V. Bakken, C. Adamo, J. Jaramillo, R. Gomperts, R. E. Stratmann, O. Yazyev, A. J. Austin, R. Cammi, C. Pomelli, J. W. Ochterski, R. L. Martin, K. Morokuma, V. G. Zakrzewski, G. A. Voth, P. Salvador, J. J. Dannenberg, S. Dapprich, A. D. Daniels, Ö. Farkas, J. B. Foresman, J. V. Ortiz, J. Cioslowski and D. J. Fox, *Gaussian 09 Revision D.01*, Gaussian Inc. Wallingford CT 2009.

43 S. H. Vosko, L. Wilk and M. Nusair, *Can. J. Phys.*, 1980, **58**, 1200.

44 C. Lee, W. Yang and R. G. Parr, *Phys. Rev. B*, 1988, **37**, 785.

45 A. D. Becke, *J. Chem. Phys.*, 1993, **98**, 5648.

46 P. J. Stephens, F. J. Devlin, C. F. Chabalowski and M. J. Frisch, *J. Phys. Chem.*, 1994, **98**, 11623.

47 K. Raghavachari, J. S. Binkley, R. Seeger and J. A. Pople, *J. Chem. Phys.*, 1980, **72**, 650–654.

48 A. D. McLean and G. S. Chandler, *J. Chem. Phys.*, 1980, **72**, 5639–5648.

49 T. Clark, J. Chandrasekhar, G. W. Spitznagel and P. von Ragué Schleyer, *J. Comp. Chem.*, 1983, **4**, 294–301.

50 T. Yanai, D. Tew and N. C. Handy, *Chem. Phys. Lett.*, 2004, **393**, 51.

51 J. Linderberg and Y. Öhrn, *Propagators in Quantum Chemistry*, John Wiley and Sons, Hoboken, New Jersey, 2004, p. 79.

52 V. G. Zakrzewski, O. Dolgounitcheva, A. V. Zakjevskii and J. V. Ortiz, *Annu. Rep. Comput. Chem.*, 2010, **6**, 79.

53 D. Zuev, K. B. Bravaya, T. D. Crawford, R. Lindh and A. I. Krylov, *J. Chem. Phys.*, 2011, **134**, 034310.

54 E. Janusson, A. Hesketh, K. Bamford, K. Hatlelid, R. Higgins and J. S. McIndoe, *Int. J. Mass Spectrom.*, 2015, **388**, 1–8.

55 M. Uppsten and B. Durbeej, *J. Comput. Chem.*, 2012, **33**, 1892–1901.

56 A. V. Bochenkova, B. Klærke, D. B. Rahbek, J. Rajput, Y. Toker and L. H. Andersen, *Angew. Chem. Int. Ed.*, 2014, **53**, 9797–9801.

57 C. W. West, J. N. Bull, A. S. Hudson, S. L. Cobb and J. R. R. Verlet, *J. Phys. Chem. B*, 2015, **119**, 3982–3987.

58 A. M. Bogdanov, A. S. Mishin, I. V. Yampolsky, V. V. Belousov, D. M. Chudakov, F. V. Subach, V. V. Verkhusha, S. Lukyanov and K. A. Lukyanov, *Nat Chem Biol*, 2009, **5**, 459–61.